

Gravitational Lensing of High Redshift Type Ia Supernovae: A Probe of Medium Scale Structure

R. Benton Metcalf

*Departments of Physics and Astronomy, and Center for Particle Astrophysics
University of California, Berkeley, California 94720*

ABSTRACT

Gravitational lensing will magnify and demagnify high redshift type Ia supernovae. The dispersion in the peak magnitudes due to this effect approaches the size of the intrinsic dispersion at $z \gtrsim 1$. A statistical method is proposed for measuring lensing's effect on the variance and the skewness of the supernova luminosity distribution. It is shown that the added dispersion is related to $a^{-2}kP(k)$ which makes it sensitive to halo scale density structure - a scale of structure that is not easily probed through observations of lensed galaxies. Using cold dark matter models it is estimated that the amount and quality of data needed is attainable in a few years. A parameterization of the signal as a power law of the angular size distance to the supernovae is motivated by these models. The signal is found to be highly dependent on scales where structure is nonlinear and weakly dependent on the Hubble parameter. The lensing's redshift dependence is related to the evolution of medium scale structure between the present and $z \sim 0.5 - 1.5$. The statistical method proposed could also be used to look for other sources of redshift evolution in the properties of type Ia supernovae.

1. Introduction

There is presently a large effort underway to predict and detect the weak gravitational lensing caused by Large Scale Structure (LSS) or the "cosmic shear" (see Valdes, Tyson & Jarvis 1983, Mould *et al.* 1994, Villumsen 1996, Kaiser 1992, Kaiser 1996). Such a measurement would constitute a direct probe of the mass density fluctuations on large scales irrespective of how light and baryons are distributed. This would make it possible to measure one of cosmology's least well understood processes, how light traces mass and whether this is a function of scale. Gravitational lensing causes images to be both magnified and demagnified as well as stretched asymmetrically (shear). Most of the methods proposed for detecting LSS lensing are based on measuring the shear in high redshift galaxy images. Although the distortions in the ellipticities of individual galaxies are expected to be small they are distorted in coherent ways. Indications of lensing are sought in the alignment of the galaxy images with the assumption that they are not intrinsically aligned. This technique has already been used with great success on galaxy cluster lensing is presently being applied to random fields in an attempt to detect the lensing effects of large scale structure. In this paper a method of detecting lensing directly through its magnification rather than shear is proposed.

The study of high redshift supernovae (SNe) is another area of cosmology and astrophysics that has seen a lot of activity lately. Type Ia SNe, the brightest type of supernova (SN), are believed to be caused by the thermonuclear explosion of an accreting white dwarf. It has been found empirically that the peak magnitude of type Ia's have a dispersion of only 0.2 - 0.3 mag in B band. It has further been found that the peak magnitude is related to the width of the SN's light-curve which can then be used to reduce the dispersion to about 0.17 mag if one color is used Hamuy *et al.* (1996) and 0.12 mag if multiple colors are used Riess, Press & Kirshner (1996). In addition to the light-curve width, the SN's color and spectral features are related to the peak luminosity (Branch, Nugent & Fisher 1997, Nugent *et al.* 1995). It may be possible to reduce the dispersion to below 0.1 mag in the future. This uniformity in type Ia SNe combined with their high luminosity makes them an excellent tool for doing cosmology. Using them to measure

the redshift-luminosity distance relation has recently resulted in tightened constraints on the cosmological parameters Ω and Ω_Λ (Perlmutter *et al.* 1997, Perlmutter *et al.* 1998, Garnavich *et al.* 1998). There are now systematic searches for Ia SNe at high redshift which can reliably discover on the order of ten SNe in two nights of observing and do spectroscopic followup Perlmutter *et al.* 1997. In addition there are several ongoing searches for low redshift SNe. To date there have been more than 100 type Ia SNe discovered with redshifts between $z = 0.4$ and 0.97 and many additional ones at lower redshift.

SNe will be magnified or demagnified by any nonhomogeneous mass distribution that happens to lie near our line of sight. Being point sources the shear in SNe images will not be observable. If the mass responsible for the lensing is in compact objects ($\gtrsim 10^{-3} M_\odot$) there is the possibility that the SNe will be microlensed. This situation was investigated by Schneider & Wagoner (1987) and Linder, Schneider & Wagoner (1988). Microlensing occurs when two images of the source are produced which are too close together to be individually resolved and can result in very high magnifications. If it occurs, the microlensing of SNe could be identifiable because the changing size of the SN's photosphere makes the magnification time dependent and thus distorts the light-curve. In addition, the peak in the distribution of magnifications is at a significantly smaller magnification (really a larger demagnification) if all dark matter is composed of large point masses as opposed elementary particles - partials whose angular Einstein ring radius is smaller than the angular size of the source or the wavelength of the observed light. This difference might be used to determine which of these cases is the right one. In this paper I concentrate on the case of elementary particle dark matter.

A SN could also be lensed by one dominant galaxy cluster or individual galaxy. There is the possibility of getting multiple observable images and high magnifications (strong lensing) in this case. It has been suggested that observing SNe behind galaxy clusters would be a way of lifting the mass sheet degeneracy that exists in shear measurements of the gravitational lensing (Kolatt & Bartelmann 1997). The likelihood of a SN at $z = 1$ being strongly lensed by a galaxy or cluster is very small unless they are specifically sought out. In general a SN will be lensed by many galaxies and larger structures that will each have a weak contribution to the total magnification. This will increase the dispersion of high redshift SNe and decrease the precision of cosmological parameter determinations. This decrease in precision has been investigated by Frieman (1997) using analytic methods and by Wambsganss *et al.* 1997 using N-body simulations. Holz & Wald (1998) calculates the lensing of point sources using numerical simulations which assume that all matter is in unclustered galaxy halos. Kantowski (1998) (and Kantowski, Vaughan and Branch 1995) does analytic calculations of this effect under the assumption that all matter is in compact objects and none of them are close enough to the line of sight to a SN to cause significant lensing. In this paper the problem will be turned around and we will ask how well the lensing itself can be determined from the SN data.

On the face of it using SNe to look for gravitational lensing by LSS has a few disadvantages and few advantages over doing it with galaxies. First, for SNe the signal to noise in each measurement can be greater. Lensing is estimated to contribute about 5 to 10% to the observed root-mean-squared ellipticity of a $z = 1$ galaxy. For SNe the variance in the lensing contribution is comparable to the intrinsic variance in the peak magnitude at this redshift. If this were the end of the story the lensing of galaxies would clearly win out due to superior numbers. But the unlensed ellipticity distribution of galaxies at high redshift is not known and can not be easily extrapolated from zero redshift galaxies. For this reason lensing must be inferred by correlations between galaxies, either between lensed galaxies or between lensed galaxies and foreground galaxies. The result is that the lensing of galaxies measures the shear averaged over a finite area on the sky. This average shear drops rapidly with increasing area and the signal to noise is reduced to something more like 1% per galaxy on the 1 deg^2 scale. This is made up for by the large number of evaluable galaxies ($\sim 10^5 \text{ deg}^{-1}$) to the extent that fluctuations in the projected mass density at $1 - 100$ arcmin scales are expected to be detectable in the near future. In contrast, the dispersion in the absolute magnitude of type Ia SNe is presumably independent of redshift. The dispersion can then be measured in a low redshift population were lensing is not important. The lensing of galaxies does have

the advantage of sources that are generally at a higher redshift where the lensing is stronger. On the other hand, the redshift of distribution of faint galaxies is not strongly constrained which adds systematic uncertainty. The redshifts of SNe are individually measured.

It is clear that the lensing of SNe and the lensing of galaxies probe different scales of density fluctuations for several reasons. Because the lensing of galaxies can only be detected through correlations in their shear, or positions and shear, lensing structures that are smaller than roughly the separation between galaxies are not detectable. Since SNe are each an independent measure of the lensing at a point, not an average over a region on the sky, they will be sensitive to smaller scale structures. Also the lensing of SNe is a direct measurement of the magnification which, in the weak lensing limit, is directly related to the mass density along the line of sight. The shear is dependent on the mass outside of the “beam” and thus a shear map is in a way a smoothed version of a surface density map. The shear and the magnification are related to each other through a differential operator (Kaiser & Squires 1993) which makes the shear insensitive to a uniform offset in the surface density - the “mass sheet degeneracy”. Although the lensing of galaxies has limitations on small scales it does have the potential of measuring lensing over a large range of scales, arcminutes to degrees. With the possible exception of SNe viewed through galaxy clusters, it will be very difficult to find enough SNe that are close enough together to measure correlations in their lensing.

In the next section I describe first how the lensing of SNe is related to the density fluctuations and then I describe how the lensing signal could be identified in the data. In section 3 specific model of structure formation is used to estimate the level of signal and to motivate some parameterizations. The last section contains conclusions and remarks about possible complications.

2. Formalism

In section 2.1 I show how the variance in the magnification of SNe is related to the power spectrum of density fluctuations in the universe. In this section only a few loose and justifiable restrictions on the form of the density fluctuations will be required. In section 2.2 a statistical method for handling the data and quantifying the lensing contributions is discussed. It is assumed throughout that the lensing is weak and multiple images are not produced. This assumption is well justified for the redshifts considered here.

2.1. Background Magnification

Here it is shown how the luminosities of SNe are affected by background mass fluctuations. It is to be expected that the variance of SN magnitudes will be increased by lensing. In addition, if two or more SNe are close enough together on the sky they will be lensing by coherent structures so their magnitudes will be correlated even if they are at different redshifts.

Lensing can be viewed mathematically as a mapping from points on a source plane to points on a image plane. The Jacobian matrix of this mapping can be written as the identity plus a perturbation, $J_{ij}(\theta) = \delta_{ij} + \Phi_{ij}(\theta)$. In the weak lensing limit the magnification is given by

$$\mu(\theta) = \det [\mathbf{I} + \Phi(\theta)]^{-1} \simeq 1 - \text{tr} \Phi(\theta) \quad (1)$$

It is standard practice to define the convergence, $2\kappa(\theta) \equiv -\text{tr} \Phi(\theta)$. The change in the magnitude of a point source is then

$$m - \bar{m} = 2.5 \log [\mu(\theta)] \simeq 2.1715 \kappa(\theta). \quad (2)$$

To calculate correlations in $\kappa(\theta)$ I will use a perturbation method based on the techniques developed in Gunn (1967), Blandford *et al.* (1991), Kaiser 1992. I will use the same notation as Metcalf & Silk (1997).

The angular deflection of an image can be written

$$\delta\theta_i(r) = -\frac{2}{g(r)} \int_0^r dr' g(r-r') \phi_{,i}(r'). \quad (3)$$

where r is the coordinate distance and $g(r) = \{R_c \sinh(r/R_c), r, R_c \sin(r/R_c)\}$ for the open, flat and closed global geometries respectively. The curvature scale is $R_c = |H_o \sqrt{1 - \Omega - \Omega_\Lambda}|^{-1}$. Subscripts with commas in front of them denote partial derivatives and $\phi(x)$ is the potential in longitudinal gauge which is the same as the dimensionless Newtonian potential in the present context. The shear tensor which measures the stretching of an infinitesimal image is given by

$$\Phi_{ij} \equiv \frac{\partial \delta\theta_i}{\partial \theta_j} = \frac{-2}{g(r)} \int_0^r dr' g(r') g(r-r') \phi_{,ij}(r'). \quad (4)$$

The coordinate distance is related to redshift by

$$r(z) = H_o^{-1} \int_0^z dz' [\Omega(1+z')^3 + (1-\Omega-\Omega_\Lambda)(1+z')^2 + \Omega_\Lambda]. \quad (5)$$

and the luminosity distance is $d_L(z) = (1+z)g(r(z))$ so that the average magnitude of a SNe is $\bar{m}(z) = M_{Ia} + 5 \log d_L(z)$.

The convergence will on average be zero, but it will be different for each SN. We need the correlation in the convergence of two sources at points θ_1 and θ_2 on the sky and at coordinate distances r_1 and r_2 .

$$\langle \kappa(\theta_1, r_1) \kappa(\theta_2, r_2) \rangle = \int_0^{r_1} dr' \frac{g(r') g(r_1 - r')}{g(r_1)} \int_0^{r_2} dr'' \frac{g(r'') g(r_2 - r'')}{g(r_2)} \langle \nabla_\perp^2 \phi(\theta_1, r') \nabla_\perp^2 \phi(\theta_2, r'') \rangle \quad (6)$$

It is useful to work in Fourier space at this point. If the potential is statistically homogeneous and isotropic the power spectrum of the potential is related to its Fourier coefficients by $P_\phi(k) = (2\pi)^3 \delta^3(\mathbf{k} - \mathbf{k}') \langle \tilde{\phi}_k \tilde{\phi}_{k'} \rangle$. The power spectrum of the potential is then related to the power spectrum of the mass density contrast by Poisson's equation, $P_\phi(k, \tau) = 9a(\tau)^{-2} \Omega_o^2 H_o^4 k^{-4} P(k, \tau)/4$ where $a(\tau)$ is the scale factor normalized to 1 at the present epoch.

The expression (6) can be significantly simplified by using an approximation that is equivalent to Limber's equation (Limber 1954). If the scales of the structures responsible for the lensing are much smaller than the distance to the source, any correlations in the radial direction will tend to wash out. This can be incorporated into the calculation by taking the correlation function of the potential to be a function of only \mathbf{x}_\perp or equivalently, the power spectrum of the potential to be a function of only k_\perp . This is a very good approximation for most realistic models of large scale structure. For a more detailed justification see the appendix of Kaiser 1992 and Metcalf & Silk (1997).

With Limber's approximation equation (6) can be reduced to

$$\begin{aligned} \langle \kappa(\theta_1, r_1) \kappa(\theta_2, r_2) \rangle &= \left(\frac{3}{2} \Omega_o H_o^2 \right)^2 \int_0^{r_1 < r_2} dr' \frac{g(r')^2 g(r_1 - r') g(r_2 - r')}{g(r_1) g(r_2)} \\ &\quad \times \int_0^\infty \frac{dk}{2\pi} a(\tau')^{-2} k P(k, \tau') J_o(g(r')|\theta_1 - \theta_2|k). \end{aligned} \quad (7)$$

where J_o is the zeroth order Bessel function. Note that no assumption of Gaussianity or linear evolution of structure has been used in deriving (7).

2.2. Measuring Parameters

The question I will address here is how to measure the parameters of a model using the SN data. And conversely, we want to know the amount and quality of the data that will be necessary to measure

parameters to a given accuracy. To do these things I use a likelihood analysis approach which begins with defining a likelihood function. The distribution of κ is not expected to be Gaussian. Nonlinear clustering causes the distribution to be skewed in favor of demagnification. This is simply because the mass is concentrated into small regions so a typical line of sight will tend to travel disproportionately through underdense regions. The distribution of corrected, intrinsic magnitudes may not be Gaussian either. At present the low redshift SNe show some evidence of skewness, but are roughly consistent with Gaussian after corrections for extinction. Extinction corrections are more difficult for high redshift SNe so non-Gaussianity may be introduced in this way as well. However one expects that the distribution of Δm will be close to Gaussian because it is the result of several independent random processes. To account for the small deviation from Gaussianity the second term of the Edgeworth expansion of the probability function is included (see for example Cramér (1946) and Juszkiewicz *et al.* (1995)). This gives the distribution a possibly measurable skewness.

The perturbed Gaussian likelihood function is

$$\mathcal{L} = \frac{1}{\sqrt{(2\pi)^n \det \mathbf{C}}} \exp\left(-\frac{1}{2} \mathbf{\Delta m}^T \mathbf{C}^{-1} \mathbf{\Delta m}\right) \prod_i \left[1 + \frac{1}{6} \mu_i^3 H_3\left(\frac{\Delta m_i}{\sigma_i}\right)\right], \quad \sigma_i^2 = 4.715\langle\kappa_i^2\rangle + (\sigma_m^2)_i \quad (8)$$

where $\Delta m_i \equiv m_i - \bar{m}_i$, the difference between the observed and expected magnitudes, and \mathbf{C} is the covariance matrix as predicted by the model. The subscripts correspond to each of the SNe observed. I will divide the covariance matrix into two parts, the first due to lensing and the second due to other sources of dispersion in SN peak luminosities - $C_{ij} = 4.715\langle\kappa_i\kappa_j\rangle(z) + (\sigma_m^2)_i \delta_{ij} + C_{ij}^{cor}$. The matrix C_{ij}^{cor} has no nonzero diagonal elements and is included to account for correlations between the SN luminosities that might arise from the light-curve and/or color corrections. The diagonal elements of C_{ij} are the σ_i 's. In turn we can divide $(\sigma_m^2)_i = \sigma_M^2 + (\sigma_n^2)_i$ where σ_M is the variance in the intrinsic peak magnitude which is the same for all SNe and $(\sigma_n^2)_i$ is the variance due to noise, light-curve fitting, etc. There is no sum over repeated indices. Maximizing (8), or its log, with respect to all the model parameters will result in the set of parameters that best fit the data. Constraints from other, independent determinations of parameters could be incorporated into the likelihood function with a prior distribution.

In (8) $H_3(x)$ is the third Hermite polynomial normalized so that

$$\int_{-\infty}^{\infty} dx H_l(x) H_m(x) e^{-x^2/2} = \begin{cases} 0 & l \neq m \\ \sqrt{2\pi} l! & l = m \end{cases} \quad (9)$$

The parameter μ_i^3 is the skewness of the Δm_i distribution. It is related to the third moment, M_i^3 , by $\mu_i^3 = M_i^3/\sigma_i^3$. The third moments of the distributions add so if both the lensing and the intrinsic Δm distributions have a third moment

$$\mu_i^3 \sigma_i^3 = 4.715\langle\kappa_i^2\rangle^{3/2} \mu_{\kappa i}^3 + \sigma_m^3 \mu_m^3. \quad (10)$$

Just like in the case of the variance, the skew due to lensing could be differentiated from the intrinsic skew by its redshift dependence. I will ignore any skew that might be in the correlation between SNe. This is likely to be small and it is not likely that it could be meaningfully constrained by observations. The maximum of the Gaussian likelihood function, $\langle \ln \mathcal{L}_{Gauss} \rangle$, is at the same place in parameter space whether the true distribution has skewness or not so, on average, the set of most likely parameters will be the same. However, the significance and shape of confidence regions will change.

If the correlations between different SNe are ignored the covariance matrix is diagonal. In section 3 it will be shown that this is a good approximation. The likelihood function simplifies in this case to

$$\ln \mathcal{L} = \frac{1}{2} \sum_i \left[(\Delta m_i)^2 (4.715\langle\kappa_i^2\rangle + (\sigma_m^2)_i)^{-1} + \ln (4.715\langle\kappa_i^2\rangle + (\sigma_m^2)_i) + \ln (1 + \mu_i^3 H_3(\Delta m_i/\sigma_i)) \right]. \quad (11)$$

Now I turn to the problem of estimating the precision with which cosmological or model parameters will be determined. The precision can be estimated by the ensemble average of the Fisher matrix which is made of the second derivatives of the likelihood function with respect to those parameters. To simplify things I will assume that the skewness, μ_i^3 , is not a function of the parameters of interest. Then if we consider two parameters α and β ,

$$\left\langle -\frac{\partial^2 \ln \mathcal{L}}{\partial \alpha \partial \beta} \right\rangle = \langle (\alpha - \bar{\alpha})(\beta - \bar{\beta}) \rangle_{\mathcal{L}}^{-1} = \text{tr} \left[\bar{\mathbf{m}}_{,\alpha} \bar{\mathbf{m}}_{,\beta}^T \mathbf{C}^{-1} + \frac{1}{2} \mathbf{C}^{-1} \mathbf{C}_{,\alpha} \mathbf{C}^{-1} \mathbf{C}_{,\beta} + \frac{1}{6} \mu_{,\alpha \beta}^3 \right]. \quad (12)$$

The first term in this expression is the usual term that comes from uncertainties in measuring the mean magnitude of the SNe and the second term is the result of the dispersion of the magnitudes, due to lensing or other things, being a function of the parameters being measured. If the SNe are taken to be statistically independent (12) simplifies to

$$\langle (\alpha - \bar{\alpha})(\beta - \bar{\beta}) \rangle_{\mathcal{L}}^{-1} = \sum_i (4.715 \langle \kappa_i^2 \rangle + (\sigma_m^2)_i)^{-2} \left\{ \bar{m}_{i,\alpha} \bar{m}_{i,\beta} (4.715 \langle \kappa_i^2 \rangle + (\sigma_m^2)_i) + \frac{(4.715)^2}{2} \langle \kappa_i^2 \rangle_{,\alpha} \langle \kappa_i^2 \rangle_{,\beta} \right\}. \quad (13)$$

We can also find the estimated uncertainty in the skewness. To first order in μ_i^3 , $\langle (\mu_i^3 - \langle \mu_i^3 \rangle)^2 \rangle^{-1} = N_i$.

3. Scalings, Models and Predictions

To make some quantitative and qualitative estimates I use models whose mass density is dominated by cold dark matter (CDM). It is helpful to first consider what might be expected for the form of the lensing signal. In linear theory $P_L(k, a(\tau)) \propto [a(\tau)g(\Omega(\tau), \Omega_\Lambda(\tau))]^2$ where $g(\Omega, \Omega_\Lambda)$ is given in (Carroll, Press & Turner 1992). This allows the integral in (7) to decouple so that factors dependent on the power spectrum can be separated from factors dependent on cosmological parameters. The same thing happens in the opposite extreme when structure is highly nonlinear and fully virialized. In this case structure is stable in real space and the power spectrum evolves like $P_{NL}(k, a(\tau)) \propto a(\tau)^3$ regardless of cosmological parameters. These two extreme cases can be explicitly calculated for the $\Omega = 1$ model where $P_L(k, a(\tau)) \propto a(\tau)^2$,

$$\langle \kappa(z)^2 \rangle = \frac{3}{40} (r(z)H_o)^3 H_o \int_0^\infty \frac{dk}{2\pi} k P(k) \times \begin{cases} 1 & \text{linear evolution} \\ 1 - \frac{1}{2}r(z)H_o + \frac{1}{14}[r(z)H_o]^2 & \text{stable evolution} \end{cases} \quad (14)$$

where the power spectrum is evaluated at the present day. These two results bracket the real result for $\Omega = 1$ models - linear evolution bounds it at the top and stable evolution on the bottom. The same thing can be done for $\Omega \neq 1$ models. In this way if $\langle \kappa^2 \rangle$ is measured firm bounds on the integral of $kP(k)$ can be found within a model. The model will already be strongly constrained by $\bar{m}(z)$ and other observations. If the redshift dependence of $\langle \kappa^2 \rangle$ could be firmly established insight into the evolution of clustering would be gained. For $\Omega \neq 1$ models $P_L(k, a(\tau))$ is a somewhat steeper function of $r(z)$ because of the decay of potential fluctuations. The stable clustering case is less strongly dependent on Ω except for the Ω^2 factor in (7) which comes from Poisson's equation. The geometric factors in $\Omega + \Omega_\Lambda \neq 1$ models will tend to make $\langle \kappa(r)^2 \rangle$ steeper, all other things being equal.

To make things more quantitative I use the linear power spectrum of matter fluctuations given by (Sugiyama 1995):

$$P(k) = Ak^n T(ke^{\Omega_b + \Omega_b/\Omega}/\Omega h^2)^2 \quad (15)$$

$$T(q) = \frac{\ln(1+2.34q)}{2.34q} [1 + 3.89q + (16.1q)^2 + (5.46q)^3 + (6.71q)^4]^{-1/4}$$

To convert this to a nonlinear power spectrum I use the technique of Peacock & Dodds (1996) which is based on N-body simulations and thus does not take into account any hydrodynamics that could be

important on small scales. In all calculations $\Omega_b = 0.015h^{-2}$. This power spectrum goes to k^{-3} at small scales so that the dimensionless power spectrum $k^3 P(k)$ becomes scale independent. Figure 1 shows what range in k -space is responsible for lensing in these models. The power spectrum in this range is speculative because the Peacock & Dodds (1996) formulae which are fits to N-body simulations become less certain at small scales. I choose to cut the power spectrum off at $k = 1000 \text{ Mpc}^{-1}$ for the purposes of (7). A cutoff at $k = 100 \text{ Mpc}^{-1}$ reduces $\langle \kappa^2 \rangle$ by $\sim 10 - 18\%$.

I have found a convenient fit to the variance of the convergence in these models

$$\langle \kappa(z)^2 \rangle \simeq \eta_o^2 [r(z, \Omega, \Omega_\Lambda) H_o]^\gamma \quad (16)$$

where $r(z, \Omega, \Omega_\Lambda)$ is the coordinate distance. This fits all the $k < 1000 \text{ Mpc}^{-1}$, cluster-normalized CDM models reasonably well with $\gamma \simeq 2.92$ for flat models and $\gamma \simeq 2.80 + 0.11\Omega$ for $\Omega_\Lambda = 0$ models as is shown in figure 2. The constant η_o depends on how the power spectrum is normalized. If it is normalized to cluster abundances using the formulae of (Viana & Liddle 1996) with $h = 0.6$ I get $\eta_o^2 \simeq (0.70 + 1.44\Omega^2)h \times 10^{-2}$ for $\Omega_\Lambda = 0$ models and $\eta_o^2 \simeq (0.32 + 1.80\Omega^2)h \times 10^{-2}$ for flat models. In general the convergence does not have a simple dependence on H_o because both the power spectrum's normalization and shape are dependent on it. If the normalization is kept constant and Ω is varied independently, η_o is a steeper function of Ω , but this normalization will always be inconsistent with other observations for some range of Ω . To properly incorporate independent constraints on the normalization (or any other parameter), a prior distribution should be incorporated in the likelihood function, (8). As is expected from the discussion above, $\langle \kappa(z)^2 \rangle$ falls somewhere between stable and linear evolution for all the models.

Figure 3 shows the angular dependence of $\langle \kappa(\theta_1)\kappa(\theta_2) \rangle$. The correlations between SNe will be very small if they are separated by more than about an arc-minute. It is unlikely that enough SNe can be found close enough together for this cross-correlation to be measured. The large angular sizes and high densities of galaxy clusters make them an exception to this rule, but a random line of sight is not likely to pass through a cluster. If these cross-correlations could be measured it would be sensitive to density structures of a larger scale than the diagonal elements, $\langle \kappa_i^2 \rangle$.

To estimate how well η_o can be measured we can use (13) to find

$$\langle (\eta_o - \langle \eta_o \rangle)^2 \rangle_{\mathcal{L}}^{-1} = \frac{1}{2} \sum_i \left[\frac{9.43\eta_o(r_i H_o)^\gamma}{4.715\eta_o(r_i H_o)^\gamma + \sigma_m^2} \right]^2. \quad (17)$$

Table 1 gives estimates of the numbers of SNe needed to make a 2σ detection of $\langle \kappa^2 \rangle$ calculated using (13). The SNe are taken to all be at the same redshift, $z = 0.5$, $z = 1.0$ and $z = 1.5$. The numbers $N_{0.10}$ and $N_{0.13}$ are for $\sigma_m = 0.10$ and 0.13 . The number goes as σ_m^4 so it is very sensitive to this parameter. The models are intended to span the range that is consistent with cluster abundances and determinations of H_o .

Of course the SNe will not all be at the same redshift and the “intrinsic” variance, σ_m , in the SN magnitudes will not be perfectly determined. It makes sense to try to determine both σ_m and η_o at the same time. One way to visualize how well this could be done is to plot $\langle \ln \mathcal{L}(\eta_o, \sigma_m) \rangle$. The curves at 0.5 and 2 less than the maximum are estimations of the boundaries of the 68% and 95% confidence regions. This is plotted in figure 4. The redshift distribution of the SNe is taken to be proportional to comoving volume with a cutoff at $z = 1.3$. This is an idealization which assumes that the observed SN rate and the detection efficiency are not functions of redshift. A separate population of 25 $z \simeq 0$ SNe is also included because searches for low redshift SNe are done by targeted observations as opposed to searches for high redshift SNe which can be done either by cataloging galaxies or by differencing multiple observations of more or less random fields. Figure 5 illustrates how going to higher redshift can help in differentiating between models. The σ_8 normalizations given in figure 4 and 5 are for the linear power spectra. Changes in the linear normalization are magnified in the nonlinear power spectrum so that they show up strongly in the lensing. This can be seen in the $\sigma_8 = 0.8$, $\Omega = 1$ model which is still consistent with cluster abundances.

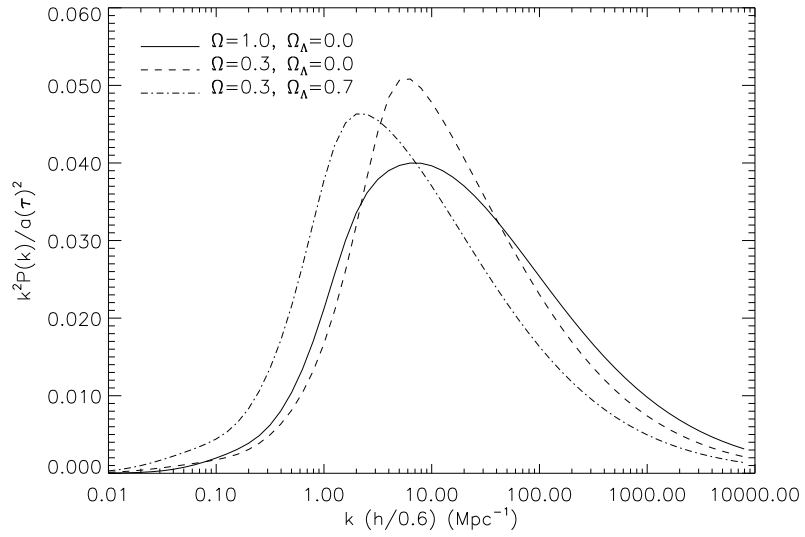


Fig. 1.— The scale dependence of the lensing of point sources in CDM models.

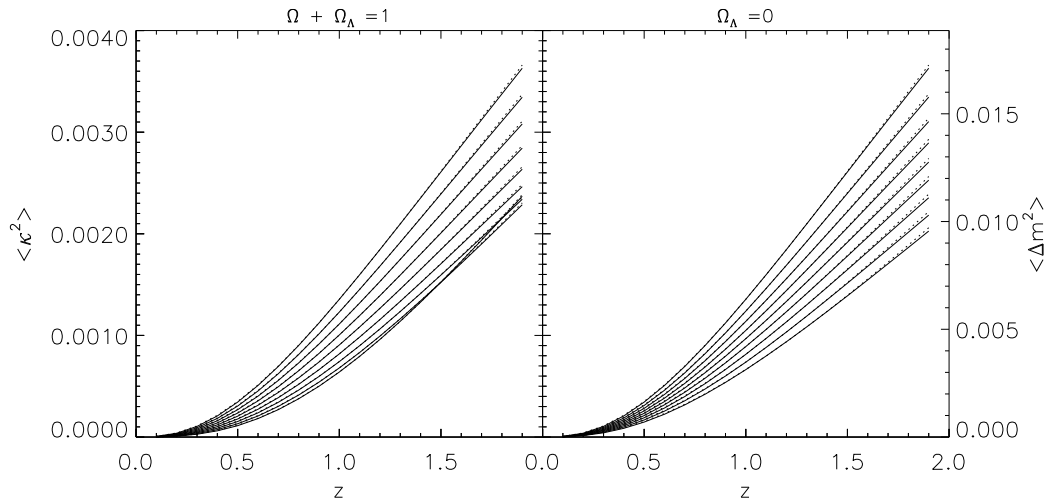


Fig. 2.— The second moment of κ in CDM models. On the left are flat models and on the right, open models. The dotted curves are the fits given in the text. The top curve in each plot is for $\Omega = 1$. Each successive curves going down has Ω reduced by 0.1 from the one above it. All the models have the normalization that best fits galaxy cluster abundances and $h = 0.6$.

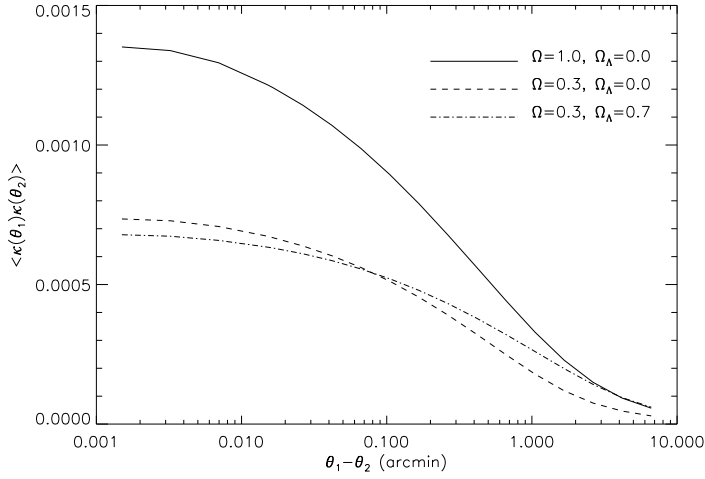


Fig. 3.— The second moment of the convergence as a function of angular separation between sources. All cases are for cluster normalized CDM models with $h = 0.6$ and the sources are at $z = 1$.

Table 1. Number of SNe Needed for Detection

Model				$z = 0.5$			$z = 1.0$			$z = 1.5$		
Ω	Ω_Λ	σ_8	h	Δm	$N_{0.10}$	$N_{0.13}$	Δm	$N_{0.10}$	$N_{0.13}$	Δm	$N_{0.10}$	$N_{0.13}$
1.0	0.0	0.6	0.60	0.04	103	261	0.08	13	27	0.11	7	11
1.0	0.0	0.6	0.75	0.05	62	153	0.09	9	17	0.13	5	8
1.0	0.0	0.5	0.65	0.03	252	668	0.06	26	59	0.09	11	22
1.0	0.0	0.8	0.65	0.06	33	76	0.11	6	10	0.16	4	5
0.3	0.0	1.0	0.60	0.03	370	995	0.06	30	69	0.08	11	23
0.3	0.0	1.0	0.75	0.03	261	694	0.06	23	50	0.09	9	17
0.3	0.0	0.7	0.65	0.02	1456	4031	0.04	97	246	0.06	31	70
0.3	0.0	1.4	0.65	0.04	89	223	0.09	10	20	0.13	5	8
0.3	0.7	1.2	0.60	0.02	592	1611	0.06	34	79	0.08	11	22
0.3	0.7	1.2	0.75	0.03	432	1165	0.06	26	59	0.09	9	18
0.3	0.7	0.8	0.65	0.02	2419	6748	0.04	114	291	0.06	31	72
0.3	0.7	1.6	0.65	0.04	139	361	0.08	11	23	0.13	5	8

Note. — These are 2σ detection limits. $N_{0.10}$ and $N_{0.13}$ refer to the number of SNe needed if $\sigma_m = 0.10$ and 0.13.

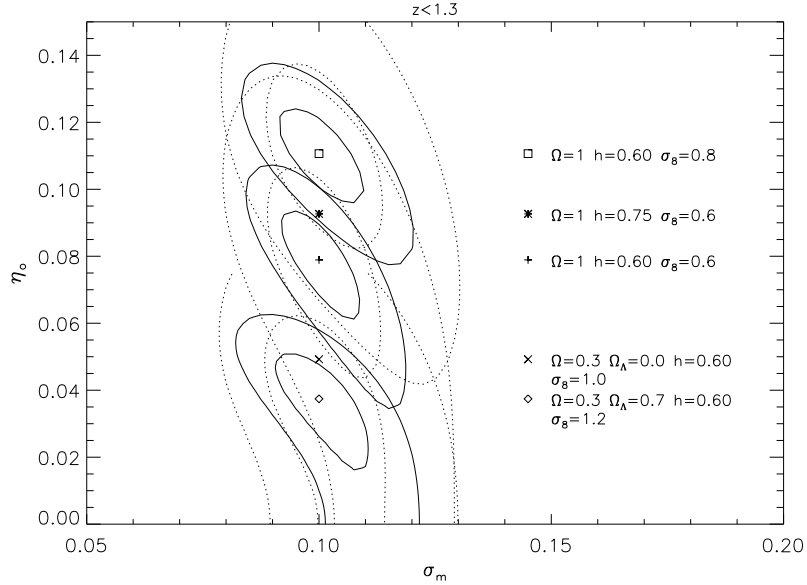


Fig. 4.— The estimated confidence regions for the combination of lensing and “intrinsic” variance in the SNe magnitudes. Solid curves are for 68% and 95% confidence regions with 25 zero redshift and 250 high redshift SNe. The dotted lines are the same for 25 zero redshift and 50 high redshift SNe. The high redshift SNe are distributed according to comoving volume with none having a redshift exceeding $z = 1.3$.

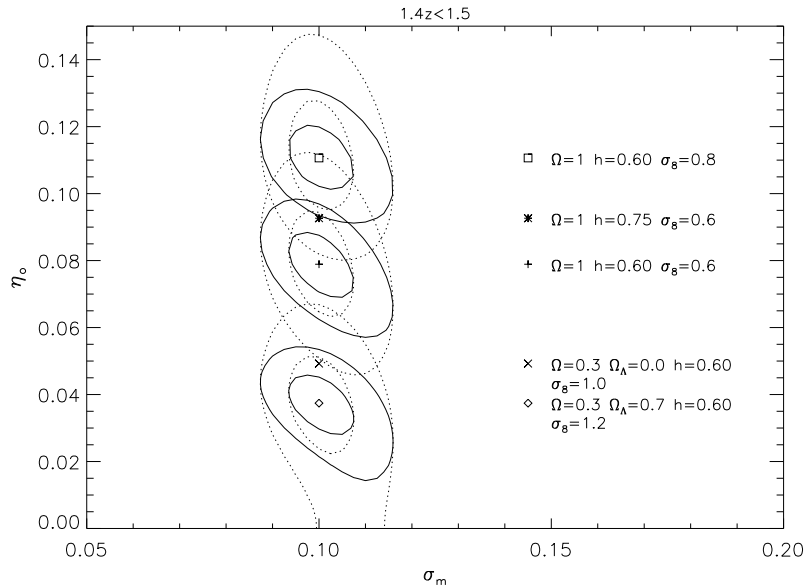


Fig. 5.— Same as in figure 4, but with 50 (dotted) and 150 (solid) SNe between $z=1.4$ and $z=1.5$. In both cases there are 100 zero redshift SNe.

Low Ω models have significantly lower η_o 's than high Ω with the same linear normalization or with cluster normalization which increases with lower Ω . This is largely because of the factor of Ω^2 in $\langle \kappa^2 \rangle$. Models with the same Ω but different Ω_Λ are not strongly discriminated between. Getting to high redshift will be important for discriminating between models because the higher the redshift the less elongated the likelihood contours are along the η_o axis. Figures 4 and 5 show that simple estimates, like the ones in table 1, that do not take into account the fact that our knowledge of σ_m is limited for a finite number can give deceptive answers. More sources are needed to detect lensing because increasing σ_m can make a lower $\langle \eta_o^2 \rangle$ acceptable.

The rate at which high redshift SNe can be discovered is limited by the rate at which they occur, the area on the sky that is surveyed and the efficiency with which they can be detected. Although the rate of star formation at high redshift can be estimated from observations (Madau *et al.* 1996), the type Ia SNe are expected to lag significantly behind it. The amount of time required for a white dwarf to accrete enough material to go SN is not only unknown, but probably varies greatly on a case to case basis. There is one measurement of the Ia SN rate at $z \sim 0.4$ which is $34.4^{+23.9}_{-16.2} \text{ yr}^{-1} \text{deg}^{-2}$ (Pain *et al.* 1996). If the rest frame rate per comoving volume remains constant the observed rate of SNe at z is $R(z) = R_o(1+z_o)g(r(z))^2/(1+z)g(r(z_o))^2$ which makes it 2 or 3 times larger at $z = 1$. More thoughtful estimations predict that the rest frame rate per comoving volume will go up by a factor of 1 to 2.5 (Sadat *et al.* 1997, Ruiz-Lapuente & Canal 1998). A SN must be detected within about a one week window in order for it to be usable. So it is reasonable to estimate that there are $\sim 20 - 50$ usable type Ia SNe per deg^2 below a redshift 1.5 at any given time. This makes detecting hundreds of high redshift SNe possible within a few years if difficulties with spectroscopic confirmation and k-corrections can be overcome.¹

These calculations of $\langle \Delta m^2 \rangle$ agree well with those of Frieman (1997). The numerical simulations of (Wambsganss *et al.* 1997, Wambsganss *et al.* 1998) give somewhat smaller values. This is probably due to the combination of their using the COBE normalization which is smaller than the cluster normalization for low Ω models and their simulation having a resolution of $\sim 13h^{-1} \text{ kpc}$ ($k \sim 480h \text{ Mpc}^{-1}$).

4. Conclusions

It has been shown that measuring the gravitational lensing of type Ia SNe is feasible if the noise can be reasonably constrained. It would be best to solve for the best fit cosmological parameters (ie. Ω , Ω_Λ), lensing strength (ie. η_o) and intrinsic noise (σ_M) simultaneously using SNe at all redshifts. The photometric uncertainties should be comparatively well determined for each SN. One could then marginalize over the intrinsic variance, σ_M . The covariance matrix C_{ij}^{cor} which expresses the correlations between SNe induced by the luminosity corrections would be best estimated by boot strapping the data. If the set of SNe used to calibrate the luminosity corrections is included in the set used to find cosmological and lensing parameters significant cross correlations could exist.

The greatest worry is of course that the type Ia SNe properties or their galactic environments are changing with redshift. Observations of spectral features and colors Perlmutter *et al.* 1997 along with theoretical models for the explosion mechanism suggest that this should not be the case, but the possibility remains. Perhaps the greatest worry for cosmological parameter estimation is extinction which will systematically reduce $\bar{m}(z)$, increase its dispersion and make its distribution non-Gaussian. Extinction should be accompanied by reddening which could be detected by observing in multiple colors, but the extinction law is not certain. The methods discussed here can be directly applied to detecting any redshift dependent change in the dispersion. With a model for how lensing changes as a function of redshift and

¹The Supernova Cosmology Project Perlmutter *et al.* 1997 currently surveys $\sim 3 \text{ deg}^2$.

the prediction that it will be uncorrelated with the spectrum or light curve of the SNe it is hoped that any other evolution could be distinguish from lensing.

There are some technical difficulties that put limits on the range of redshifts that are presently accessible for a SN search. The region of the spectrum that is used to do the light curve correction passes out of the visible at $z \gtrsim 1$. To go to significantly higher redshift may require switching to the IR. There is also some uncertainty in the K-correction. But with all this in mind it seems that gravitational lensing of SNe could be detectable in the next few years when hundreds of high redshift SNe are observed and systematic effects are better understood. CCD cameras with fields of view approaching a square degree and very small pixel sizes are being built now. They will be used for weak lensing measurements using galaxy shear. SNe searches could be incorporated into these surveys with the benefits of improved cosmological parameter estimation and complimentary weak lensing measurements.

Combined with the limits on the cosmological parameters the lensing of SNe can constrain the power spectrum of the true mass density, unbiased by the light distribution, on the scale of galaxy halos. At present the mass distribution on these scales is not well known with the exception of within galaxy clusters which are certainly atypical regions. In this paper it has been assumed that the the large majority of matter in the universe is in the form of WIMPS or some other small particle. If the dark matter is in compact objects like MACHOs the distribution of magnifications will be different. It would be likely that none of the observed SNe are significantly lensed by one of these objects. In this way the lensing of SNe also provides information on the composition of dark matter. In addition to the variance of the magnification distribution the skewness would provide an important constraint on the nature of structure in the nonlinear regime. Estimates of the skewness require more sophisticated simulations than have been used for this paper. A future paper will treat this subject in more detail and relate the skewness to the nature of dark matter and the structure of galaxy halos.

I would like to thank J. Silk, A. Jaffe, S. Perlmutter and R. Pain for very useful discussions. This work was financially supported by NASA.

REFERENCES

Blandford,R.D, *et al.*, 1991, MNRAS, 251, 600.

Branch D., Nugent P. & Fisher A., 1997, *Thermonuclear Supernovae*, ed. P. Ruiz-Lapuente, R. Canal & J. Isern (Dordrecht:Kluwer), 715.

Carroll S.M., Press W.H. & Turner E.L., 1992, ARA&A, 30, 499.

Cramér H., 1946, *Mathimatical Methods of Statistics* (Princeton:Princeton Univ. Press).

Frieman J.A., 1997, Comments on Astrophysics, 18, 323.

Gunn, J.E., 1967, ApJ, 150, 737.

Garnavich, P.M. *et al.*, 1998, ApJ, 493, L53.

Hamuy M., Phillips M.M., Suntzeff N.B., Schommer R., Maza J. & Aviles R., 1996, ApJ, 112, 2391.

Juszkiewicz R. *et al.*, 1995, ApJ, 442, 39.

Holz D.E. & Wald, R.M., astro-ph/9708036.

Kaiser, N., 1992, ApJ, 388, 272.

Kaiser, N., 1996, submitted to ApJ, astro-ph/9610120.

Kaiser, N. & Squires G., 1993, ApJ, 404, 441.

Kantowski R., 1998, astro-ph/9802208.

Kantowski R., Vaughan T. & Branch D., 1995, ApJ, 447, 35.

Kolatt T.S. & Bartelmann M., 1997, astro-ph/9708120.

Limber, D.N., 1954, ApJ, 119, 665.

Linder E.V., Schneider P. & Wagoner R.V., 1988, ApJ, 324, 786.

Madau P. *et al.* 1996, MNRAS, 283, 1388.

Metcalf, R B & Silk, J, 1997, ApJ, 489, 1.

Mould, J. *et al.*, 1994, MNRAS, 271, 31.

Nugent P., Phillips M., Baron E., Branch E. & Hauschildt P., 1995, ApJ, 455, L147.

Pain R. *et al.*, 1996, ApJ, 473, 356.

Peacock J.A. & Dodds S.J., 1996, MNRAS, 280, L19.

Perlmutter S., *et al.*, 1997, ApJ, 483, 565.

Perlmutter S., *et al.*, 1998, Nature, 391, 51.

Pozzetti L., Bruzual A.G. & Zamorani G., 1996, MNRAS, 281, 953.

Ruiz-Lapuente P. & Canal R., 1998, astro-ph/9801141.

Riess A.G., Press W.H. & Kirshner R.P., 1996, ApJ, 473, 88.

Sadat R., Blanchard A., Guiderdoni B. & Silk J., 1997, astro-ph/9712065.

Schneider P. & Wagoner R.V., 1987, ApJ, 314, 154.

Sugiyama N., 1995, ApJS, 100, 281.

Valdes F., Tyson J. & Jarvis J., 1983, ApJ, 271, 431.

Viana, P.T.P. & Liddle, A.R., 1996, MNRAS, 281, 323.

Villumsen J.V., 1996, MNRAS, 281, 369.

Wambsganss J., Cen R., Xu G., & Ostriker J.P., 1997, ApJ, 475, L81.

Wambsganss J., Cen R., & Ostriker J.P., 1998, ApJ, 494, 29.